Pichler, Thomas ; Mozaffari, Ali

Distribution and mobility of geogenic molybdenum and arsenic in a limestone aquifer matrix

Journal Article as: peer-reviewed accepted version (Postprint)

DOI of this document*(secondary publication): https://doi.org/10.26092/elib/3219

Publication date of this document: 15/08/2024

* for better findability or for reliable citation

Recommended Citation (primary publication/Version of Record) incl. DOI:

Thomas Pichler, Ali Mozaffari, Distribution and mobility of geogenic molybdenum and arsenic in a limestone aquifer matrix, Applied Geochemistry, Volume 63, 2015, Pages 623-633, ISSN 0883-2927, https://doi.org/10.1016/j.apgeochem.2015.08.006.

Distribution and mobility of geogenic molybdenum and arsenic in a limestone aquifer matrix

Thomas Pichler*, Ali Mozaffari

Geochemistry and Hydrogeology, Department of Geosciences, University of Bremen, Klagenfurter Straße, 28359 Bremen, Germany

Keywords:
Geogenic
Arsenic
Molybdenum
Aquifer matrix
Limestone
Groundwater

1. Introduction

Molybdenum (Mo) is considered an essential element, whose daily requirement for humans is approximately 0.3 mg (WHO, 2011), while at the same time high doses of Mo could be detrimental to human health. The recommendation by the World Health Organization (WHO) for drinking water is that Mo should not exceed 70 μg/L (WHO, 2011). Currently only anthropogenic Mo contamination seems to be of environmental interest and particularly in mining areas it is a well-known contaminant (Davies et al., 2005; Heijerick et al., 2012; Smedley et al., 2014; Zhai et al., 2013) where it is released during mining operations and due to weathering of mine tailings (Price et al., 1999). The deterioration of groundwater, however, is not exclusively due to the direct input of anthropogenic contaminants, such as the discharge of Pb due to battery recycling (e.g., Pichler, 2005). Another process leading to

* Corresponding author.
E-mail address: pichler@uni-bremen.de (T. Pichler).

groundwater deterioration can be the mobilization of naturally occurring (geogenic) elements induced by anthropogenic perturbations of the physicochemical conditions in the aquifer (e.g., Amini et al., 2008; Ferguson and Gavis, 1972; Korte and Fernando, 1991; McNeill et al., 2002; Peters and Blum, 2003). This type of anthropogenic-induced contamination is a public health issue worldwide. In particular the ongoing catastrophic problems with arsenic (As) in Bangladesh and West Bengal are front-page stories in newspapers and scientific journals (e.g., Ahmed et al., 2006). There is the potential that geogenic Mo could be candidate for anthropogenic-induced widespread groundwater contamination as well. Marine sediments are known to accumulate Mo in organic matter (e.g., Tribovillard et al., 2004) and in pyrite (e.g., Helz et al., 2011, 1996). Since As is known to accumulate in the same two phases the physicochemical conditions that cause the release of As from the aquifer matrix should also release Mo.

Elevated arsenic (As) is a well-known problem in Floridan groundwater, whenever the physicochemical conditions in the aquifer are perturbed due to anthropogenic activities (Arthur et al., 2007; Jones and Pichler, 2007; Katz et al., 2009; Wallis et al., 2011). Thus As is routinely analyzed after completion of new wells, which led to the discovery of elevated As and Mo concentrations in groundwater in a rural area in central Florida (Pichler and Sültenfuß, 2010). There As concentrations of up to 350 μg/L and Mo concentrations of up to 5000 μg/L were measured. The value of 5000 μg/L is substantially above what could be considered "normal" for Mo concentrations in groundwater. Smedley et al. (2014) who studied Mo in Great Britain found a 10 to 90th percentile range of 0.08–2.44 μg/L with a median of 0.57 μg/L and a maximum observation of 230 μg/L in stream water samples (n = 11,600). In groundwater samples the 10 to 90th percentile ranged from 0.035 to 1.80 μg/L with a median of 0.20 μg/L and a maximum observation of 89 μg/L (n = 1735).

While some information about the occurrence and distribution of As in the Floridan aquifer matrix exists (e.g., Pichler et al., 2011), next to nothing is known about Mo. In this study, we present a first look at the distribution and mineralogical association of As together with Mo in a limestone aquifer of marine origin. To estimate As and Mo mobility, a modified extraction was carried out according to the procedure recommended by Pichler et al. (2001).

2. Study area

The study area is located in the municipality of Lithia southeast of Tampa Bay in the United Sates (Fig. 1). There, a multilayered aquifer system exists, which can be subdivided into three distinct hydrostratigraphic units, which are, from the top down: the Surficial Aquifer System (SAS), the Intermediate Aquifer System (IAS), and the Upper Floridan Aquifer System (UFA). Katz et al. (2007) provided detailed mineralogical and lithological descriptions of these units and their regional hydrogeology in central Florida, which were recently reviewed (Hughes et al., 2009). Relevant hydrogeological characteristics of these units are briefly summarized here.

The unconfined SAS consists of unconsolidated to poorly indurated clastic deposits with depths to the water table ranging from about 3 m to 15 m below land surface (Katz et al., 2009). The upper surface of the SAS is defined by the surface topography, which near the wells with high As concentrations is generally about 30 m above mean sea level (amsl) and ranges from about 65 m just to east of the high-As wells to near zero where it intersects Hillsborough Bay about 35 km to the west. Near the high-As concentration wells, the base of the SAS is 10 m amsl and dips to the west at a slope of approximately 0.001. The SAS generally is not used as a major source of water supply because of relatively low yields (less than 19 L/min), high Fe content, and the potential for contamination from the surface. Water table elevations in the SAS generally are above the potentiometric surface of the UFA, indicating downward groundwater flow through the IAS from the SAS to the UFA (Katz et al., 2009).

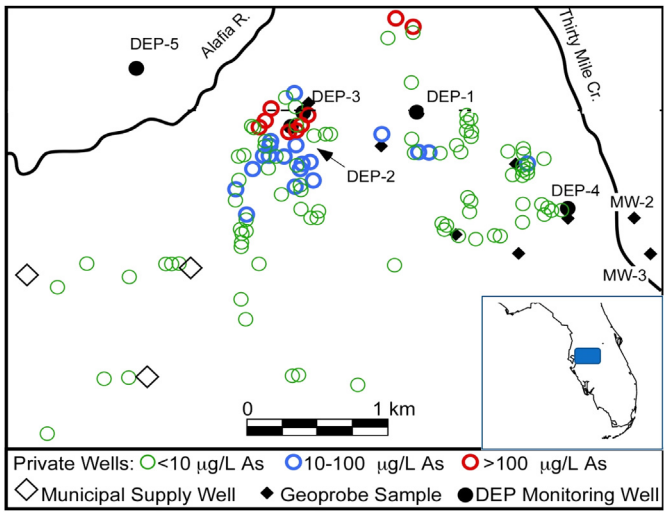

Fig. 1. Location of the study area showing domestic supply wells and their approximate As concentrations and the locations of the three cores, which were sampled for this study (DEP-1, DEP-2 and DEP-5).

The IAS consists of several water-bearing units separated by confining units, which are composed mainly of the siliciclastic Hawthorn Group with interlayered sequences of more and less permeable carbonates, sands and clays (Scott, 1988, 1990). The extent, thickness, and permeability of the IAS are variable, but generally control the downward leakage between the SAS and the UFA (Katz et al., 2009). Pyrite is found unevenly distributed throughout the Hawthorn Group and occurs mainly in its framboidal form (Lazareva and Pichler, 2007). Arsenic concentrations in the Hawthorn Group are generally less than 5 mg/kg, but can reach up to 69 mg/kg in samples with abundant pyrite (Lazareva and Pichler, 2007; Pichler et al., 2011). Near the highest As concentrations, the bottom of the IAS is about −30 m amsl and dips to the west at a slope of approximately 0.001.

The UFA is the major source of water supply within the study area and consists of permeable limestone and dolomite deposited in a shallow marine environment (Green et al., 1995; Miller, 1986). Carbonate deposition was interrupted at first periodically, and finally completely, with the influx of the siliciclastic sediments eroded from the Appalachian Mountains that form the IAS. Within the region of high As concentrations, the bottom of the UFA is about − 400 m amsl and dips to the west at a slope of approximately 0.001. Because of its high permeability, the Florida Geological Survey has been testing the UFA to serve as an underground reservoir for aquifer storage and recovery (ASR) systems. Detailed lithological, mineralogical, and geochemical studies of the two uppermost formations of the UFA, the Tampa Member and the Suwannee Limestone, showed that As is generally present in low concentrations (a few mg/kg), but is concentrated in minor minerals, such as pyrite, which may contain up to 11,200 mg/kg As (Lazareva and Pichler, 2007; Price and Pichler, 2006). The Tampa Member of the Arcadia Formation hydrostratigraphically belongs to the UFA, although it is the lowermost stratigraphic unit of the Hawthorn Group (Miller, 1986).

3. Materials and methods

3.1. Core description

To assess the occurrence, distribution and mineralogical association of As and Mo in the aquifer matrix in the study area three cores were analyzed (Fig. 1). Core DEP-1 was drilled inside the area of contamination to a depth of 114 m below surface and sampled between 44 m and 114 m. Core DEP-2 was drilled inside the area of contamination to a depth of 103 m below surface and sampled between 4 and 103 m. As a reference, core DEP-5 was drilled outside the area of contamination to a depth of 103 m below surface and sampled between 27 m and 103 m. The cores were described in detail, which included the chemical analyses for total organic carbon (TOC), Ca, Mg, Si, Al, P, Sr, As, Mo, Fe, and S content and the preparation of thin sections. Each core was sampled at a spacing of approximately 0.5 m to ensure representation of all stratigraphic units. In addition to those interval samples, targeted samples were taken along each core from sections with visible pyrite, hydrous ferric oxide, clays, or organic material. These sections were suspected to have higher As concentrations than the bulk carbonate or clay matrix. This sampling approach was successfully applied to assess the importance of pyrite as the source of As in the UFA (Lazareva and Pichler, 2007; Pichler et al., 2011; Price and Pichler, 2006). The samples were dried at room temperature and subsequently powdered and dissolved using a digestion method modified from van der Veen et al. (1985). Once cooled, the digestates were diluted to 50 mL with deionized water (DI) and allowed to settle for at least 24 h before being passed through a 2.0 μm Teflon filter. Two mL of the filtered samples were diluted with 8 mL of DI for determination of Ca, Mg, Si, Al, P, Sr, Mo, Fe, and S on a Perkin Elmer Optima 2000 DV inductively coupled plasma-optical emission spectrometer (ICP-OES). A 10 mL aliquot of each sample was prepared for As analysis by hydride generation-atomic fluorescence spectrometry (HG-AFS) on a PSA 10.055 Millennium Excalibur instrument following (Price and Pichler, 2006). To assure quality control, approximately 10% duplicate samples were randomly selected. Sample blanks, which were added every 5–10 samples, did not show detectable concentrations of As (<0.2 μg/L). To test recovery, 2 samples from each batch were spiked in liquid form with the equivalent 25 mg/kg As before digestion. Recovery of As from the spiked samples was always between 90% and 110%.

Polished thin sections were made for 20 samples high in As and Mo for further analyses of discrete mineral phases by optical microscopy, scanning electron microscopy (SEM) using a Zeiss Supra 40 instrument equipped with a Bruker EDX detector and electron microprobe analysis (EMPA) using a JEOL JXA-8900R instrument. Reference materials consisted of natural and synthetic sulfide, sulfate, silicate, and oxide. Due to logistic limitations, only core DEP-2 was analyzed top to bottom. The other two cores, DEP-1 and DEP-5, were analyzed starting at a depth of approximately 45 m (below surface) and had essentially the same stratigraphy, element patterns and concentrations as DEP-2 (Appendix A and B).

Total carbon (TC), inorganic carbon (IC) and total organic carbon (TOC) were determined as follows: (1) The samples were dried at 105 °C, (2) TC was determined by combusting a dried sample at 1350 °C in an oxygen atmosphere using a LECO CR-412 instrument, (3) TOC was determined by the same combustion method after removal of IC with phosphoric acid (1:1) and (4) IC was determined by difference.

3.2. Mobilization test for weakly bound As and Mo

To assess the mobilization potential of As and Mo from the aquifer matrix 10 samples were chosen for a chemical extraction experiment based on the following criteria: (1) high total Mo concentration, (2) high total As concentration and (3) geographic representation of the study area (Fig. 1). The extraction experiment was carried out on duplicate samples following step 1 of an established sequential extraction procedure (Pichler et al., 2001; Price and Pichler, 2005). All chemicals used were reactant grade or better and solutions were prepared with double deionized water (DDI) of at least 18 MΩ cm^{-1}.

The purpose of this procedure was to assess the amount of exchangeable (i.e., easily mobilized) As and Mo in the aquifer matrix. To carry out the extraction 20 mL of 1.0 M sodium acetate (NaOAc) adjusted to a pH of 8.1 were added to 1 g of powdered sample in a 50 mL screw cap centrifuge tube and shaken for 2 h at room temperature in a mechanical shaker operating at 250 motions min^{-1}. The extract was separated from the solid residue by centrifugation at 4000 RPM for 10 min. The supernatant was decanted into a 50 mL tube, diluted to 50 mL and prepared for chemical analyses (i.e., filtration, dilution if necessary). To wash the residuals they were re-suspended in 5 mL of DI water then centrifuged and the supernatant was discarded.

4. Results

4.1. Stratigraphy, mineralogy and chemical composition of the cores

The stratigraphy from top to bottom was approximately as follows: 0–18 m surficial sediments (SAS), 18–60 m Hawthorn Group (IAS), 60–70 m Tampa Member (UFA) and below 70 m Suwannee Limestone (UFA). Except in the uppermost segment, limestone was the main lithology. Occasionally dolomite and clay minerals were present. That lithology was also observed in the bulk chemical composition, where Ca, Mg and Sr concentrations increased with depth, while Si, Al and P decreased, indicating the decreasing siliciclastic and clay content (Appendix A and B). Core lithology, Arsenic and Mo concentrations in DEP-5, which was the reference core from outside the area of contamination, did not differ from those cores drilled inside the area of contamination (DEP-1 and DEP-2). The minimum, maximum, median and standard deviations for all analyzed elements, including As and Mo were comparable for all three cores (Figs. 2 and 3, Appendix B). Molybdenum, As, S and Fe, however, varied significantly with depth and median As and Mo values were above their respective crustal averages of approximately 1.1 mg/kg and 1.5 mg/kg (Li, 2000). The median values for As were 3.4 mg/kg in DEP-1, 4.7 mg/kg in DEP-2 and 3 mg/kg in DEP-5 (Appendix A, Fig. 3). The median values for Mo were 4.4 mg/kg in DEP-1, 6 mg/kg in DEP-2 and 3.1 mg/kg in DEP-5 (Appendix A,

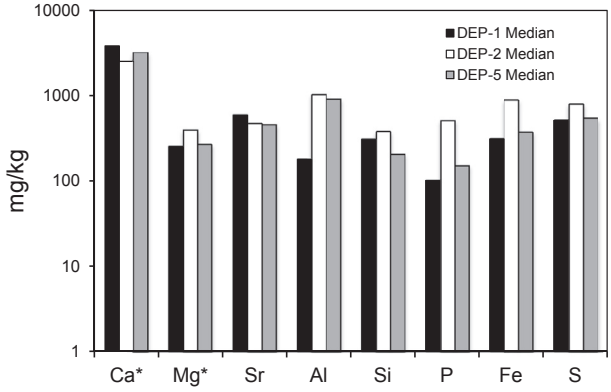

Fig. 2. Comparison of the median concentrations of Ca, Mg, Sr, Al, Si, P, Fe and S in sediments samples from the three cores DEP-1, DEP-2 and DEP-5. *To allow for better presentation Ca and Mg values were divided by 100 and 10, respectively.

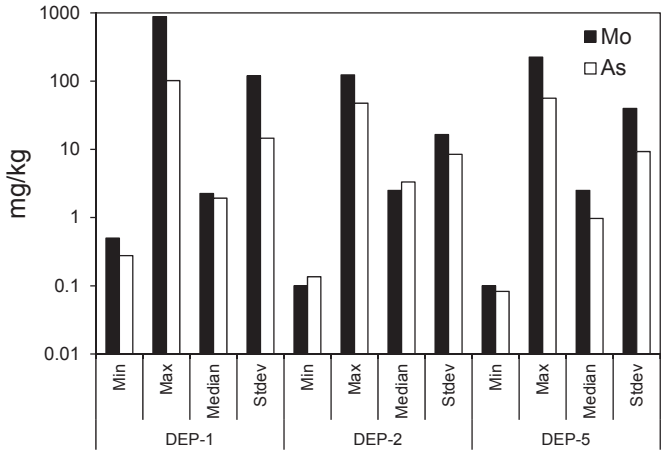

Fig. 3. Comparison of the minimum, maximum, median and standard deviations of As and Mo concentrations in sediment samples from cores DEP-1, DEP-2 and DEP-3. Although there are differences in minimum and maximum concentrations, the median values are more or less identical.

Fig. 3). However, these median values are heavily skewed due to occasionally high values of up to 100 mg/kg for As and up to 880 mg/kg for Mo (Appendix A).

The concentrations were highest in the SAS and IAS and returned to "normal", i.e., expected values for crustal carbonate rocks, in the UFA below a depth of 60–70 m below surface (Fig. 4). The concentrations of Fe and S seemed to follow the same pattern, being elevated in each of the cores at approximately the same depth (Fig. 5). In core DEP-1 As was elevated at depths of approximately 45 m and 55 m (Fig. 5). In core DEP-2 As varied significantly between 5 m and 35 m and then had two pronounced high concentrations at 45 m and 60 m (Fig. 5). In core DEP-5 As was elevated at depths of approximately 50 m and 65 m (Fig. 5). In core DEP-1 Mo was elevated at depths of approximately 45 m and 70 m (Fig. 5). In core DEP-2 Mo showed the same pattern as As. It varied significantly between 5 m and 35 m and then had two pronounced high concentrations at approximately 45 m and 70 m (Fig. 5). In core DEP-5 was elevated at several depths, the highest values at

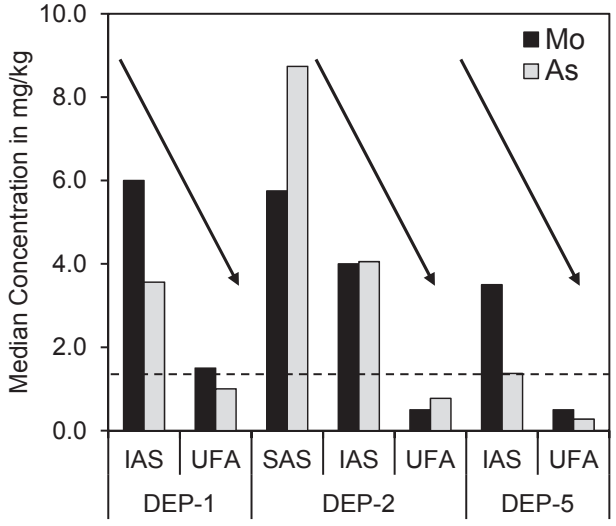

Fig. 4. Comparison of the medians of As and Mo concentrations in each hydrostratigraphic section in sediment samples from cores DEP-1, DEP-2 and DEP-3. The median values decrease with increasing depth. The dashed line approximately depicts the average concentration of As and Mo in crustal rocks.

approximately 50 m and 75 m (Fig. 5).

Euhedral and framboidal pyrite was identified as a minor mineral in the IAS and UFA sections (Fig. 6), where it generally filled void spaces. Sometimes occurring together with hydrous ferric oxide (HFO) (Fig. 6A) or with powellite (Fig. 6B). Electron microprobe analyses revealed variable concentrations of As in pyrite ranging from approximately 300 to 9000 mg/kg (Table 1). The molybdenum concentration in pyrite was consistently below the detection limit of approximately 100 mg/kg and the highest values for Zn and Sb were 806 mg/kg and 730 mg/kg, respectively. These values were in the same range as those previously reported for the IAS (Lazareva and Pichler, 2007) and Suwannee Limestone (Price and Pichler, 2006). HFO was identified mainly in the upper sections of the cores.

In core DEP-1 the calcium molybdate powellite ($CaMoO_4$) was identified at a depth of approximately 45 m. It occurred as very small grains of approximately 20 μm in diameter filling void spaces and enclosing primary mineral grains of the aquifer matrix indicating that powellite was the latest stage of mineral formation (Fig. 6B). Based on the average of 5 EMPA measurements, its chemical composition by mass was approximately 21% Ca, 42% Mo and 1.76% As, while other elements were less than 0.2% (Table 2). The elevated As concentration could also be observed by energy dispersive X-ray spectroscopy (EDX) (Fig. 6D).

Organic carbon was present throughout the cores, ranging from 0.1 to 3.3% (Appendix C). Its occurrence in each of the three cores was almost identical. Core DEP-1 had a maximum concentration of 2.6% and a median of 1.4% ($n = 22$), core DEP-2 had a maximum concentration of 3.0% and a median of 1.4% ($n = 27$) and core DEP-5 had a maximum concentration of 3.3% and a median of 1.4% ($n = 26$).

4.2. Mobilization experiment

The results for the mobilization of Mo and As are shown in Table 3. Analytical quality was evaluated by including a replicate and a blank in each analytical batch. The results showed high precision for replicate samples (average standard deviation of replicates were 2.8 for Mo and 0.86) for As and the blanks did not contain detectable concentrations of either element.

During the experiment with NaOAc at a pH of 8.1, which had the purpose to identify easily mobilized Mo in the aquifer matrix up to 97% were removed (Fig. 7). More than 80% Mo was removed from samples 45–46, 46–47, 70–71, 31–32, 42–43 and 51–52 and approximately 65%–70% Mo was removed from samples 18–19 and 75–76. Despite the high extraction from these samples, two samples 10–11 and 69–70 showed much lower Mo extraction of 5% and 21%, respectively. The percentages were calculated using the corresponding Mo concentrations from the total analyses (Appendix A).

In contrast to Mo, As was mobilized to a lesser degree and the samples could be divided into three groups. Between 21% and 50% As were removed from samples 42–43, 45–46, 46–47, 70–71 and 31–32 and approximately 10%–24% As were removed from samples and 50–51, while little to nothing was removed from the remaining samples, 10–11, 18–19 and 69–70 (Table 3). The percentages were calculated using the corresponding As concentrations from the total analyses (Appendix A).

5. Discussion

5.1. Molybdenum

In the aquifer matrix below the town of Lithia in central Florida cores, Mo was elevated in certain horizons, particularly at depths of

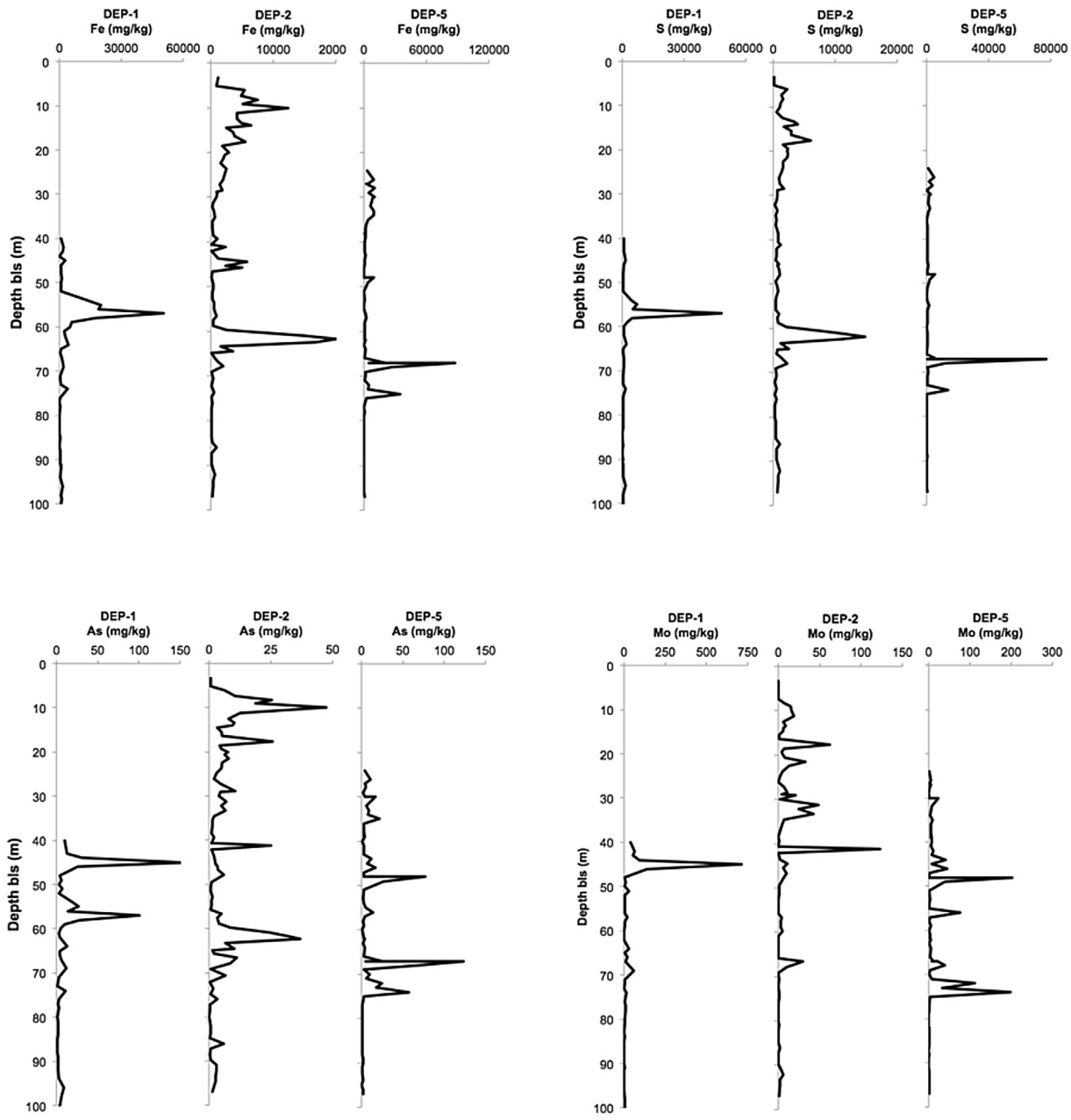

Fig. 5. Approximate stratigraphy and depth profiles for the concentration of iron (Fe), sulfur (S), arsenic (As) and molybdenum (Mo) in cores DEP-1, DEP-2 and DEP-5.

approximately 40–60 m below surface in all three cores (Fig. 5). Values were comparable between the cores with maximum values above 100 mg/kg and median values of around 3 mg/kg. These values were higher than what was considered to be the mean concentration of Mo in the Earth's crust of around 1–2 mg/kg (Li, 2000). However, Mo concentrations can be significantly higher in sediments, which were deposited under oxygen-depleted conditions. Hatch and Leventhal (1992) reported up to 850 mg/kg Mo for the Stark Shale Member of the Dennis Limestone in Kansas and Calvert and Pedersen (1993) reported a range from 21 to 160 mg/kg Mo for sediments from several anoxic basins. In purely oxic sediments of marine origin Mo concentrations are generally much lower (Bertine and Turekian, 1973; Crusius et al., 1996) and thus changing redox conditions during deposition may cause the Mo variation seen in the DEP cores (Fig. 4). According to Scott (1988) the depositional environment of the Hawthorn Group changed constantly from marine or peri-marine conditions that seemed to have ranged from prodeltaic and shallow to sub-tidal marine, to intertidal and supratidal with occasional deposition of terrestrial sediments in the form of paleosoils and weathered residuum of the Hawthorn sediments. In addition the existence of phosphorite deposits in the Hawthorn Group points towards upwelling and the associated changes in redox conditions (Riggs, 1984), as well as the varying abundance of organic carbon in the sediments (Appendix B).

The exact mineralogical association of Mo in the aquifer matrix remains unclear, although the mineral powellite ($CaMoO_4$) was observed in the aquifer matrix (Fig. 6). Based on crystal habit it is unlikely that powellite is a primary mineral that would have precipitated during sediment deposition or early diagenesis. In Fig. 6B powellite encloses primary calcite fragments indicating that it was the latest or one of the latest mineral phases to precipitate in

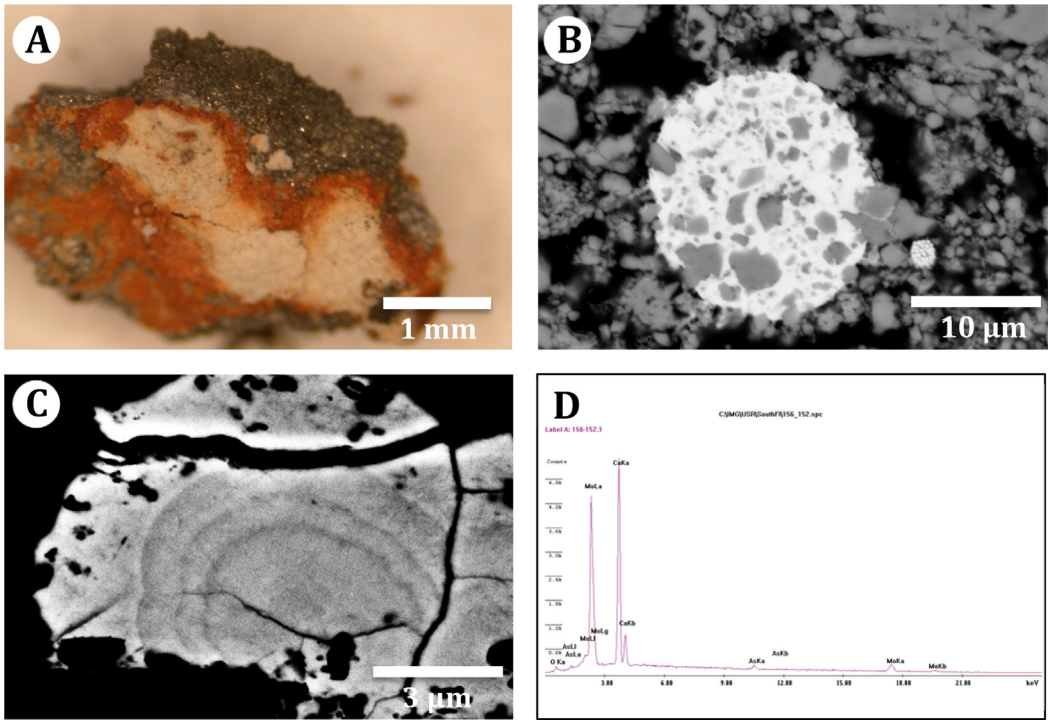

Fig. 6. (A) Optical microscopy image of pyrite and HFO in core DEP-1 at a depth of 60 m. (B) Back scatter electron image of powellite and a framboidal pyrite from core DEP-1 (46 m depth) of powellite in a clay/carbonate matrix. (C) Secondary electron microprobe image (polished thin section) of a powellite crystal showing fine growth banding. (D) EDX spectra for the powellite in image B.

the aquifer matrix. Precipitation of powellite due to evaporative concentration of Mo in the pore water during drying of the samples could have happened. However, several powellites showed very delicate banding, which appeared to be growth banding (Fig. 6C). The fine scale of the bands and their uniformity precludes the type of rapid deposition one would expect from evaporation during core handling. Thus it is conceivable that powellite is a sink for Mo, rather than a source. Thermodynamic modeling with the computer code Geochemist's Workbench (GWB), using recent thermodynamic data for aqueous Mo species, powellite and molybdenite, showed that powellite was super-saturated in groundwater samples with Mo concentrations above 2000–3000 µg/L. Precipitation of powellite from super-saturated groundwater was observed elsewhere as well (e.g., Conlan et al., 2012). Thus, the likely primary source for Mo is organic matter, which is sufficiently abundant in the aquifer matrix. The mean concentration was in each of the three cores was 1.4%, which is significantly higher than 0.24%, which is considered the mean concentration in limestone (Gehman, 1962). Organic matter has a high adsorption potential for Mo (Jenne, 1998) and is known to incorporate and concentrate Mo (e.g., Tribovillard et al., 2004).

Under reducing conditions at the time of sediment deposition, Mn refluxing has the potential to concentrate dissolved MoO_4^{2-} at the sediment–water interface. In cases where anoxia extends upward into the water column, Mn^{2+} oxidizes to particulate MnO_x (solid) just above the chemocline. The particulate Mn settles into the anoxic waters, and re-dissolved Mn^{2+} diffuses back through the chemocline, thus completing a redox cycle (Adelson et al., 2002). In this case Mo can be co-precipitated by Mn and Fe oxides. However, no evidence was found to indicate that Mo was co-precipitated with Mn and Fe oxides during time of sediment deposition. The Mn concentrations were rather low and more or less uniformly distributed throughout the study area with median values of 24, 37 and 34 for Cores DEP-1, DEP-2 and DEP-5, respectively. The possible explanation is that the physicochemical conditions in the sedimentary environment did not change sufficiently. On the other hand, in sulfidic settings, pyrite and organic matter (OM) have a greater capability to fix Mo from seawater and retain it during diagenesis (Adelson et al., 2002; Helz et al., 2011, 1996; Tribovillard

Table 1
Average chemical compositions of pyrite (FeS_2) in thin sections from cores DEP-1 and DEP-2.

Core	Sample	Fe	S	As	Sb	Zn	Mo	Ca	Total
		wt%	wt%	mg/kg	mg/kg	mg/kg	mg/kg	wt%	wt%
DEP-1	45–46	42	52	8788	730	320	<0.5	0.19	95
DEP-1	45–46b	47	52	2113	0	48	<0.5	0.53	99
DEP-1	57–58	47	52	1281	18	40	<0.5	0.04	99
DEP-1	57–58	48	53	360	0	15	<0.5	0.03	101
DEP-1	64–65b	47	53	451	9	68	<0.5	0.15	100
DEP-1	64–65	46	52	1412	16	54	<0.5	0.24	98
DEP-2	17–18a	47	53	794	9	59	<0.5	0.22	99
DEP-2	17–18b	46	52	1164	11	806	<0.5	0.39	98
DEP-2	41–42	38	51	6597	57	19	<0.5	0.52	90
DEP-2	62–63d	47	53	1846	32	28	<0.5	0.03	100
DEP-2	62–63b	47	52	1713	25	98	<0.5	0.11	99
DEP-2	67–68	46	54	681	66	21	<0.5	0.76	101
DEP-2	68–69	48	53	285	13	6	<0.5	0.06	101

Table 2
Average chemical compositions of powellite ($CaMoO_4$) in thin sections from core DEP-1.

Core	Sample	Fe	S	As	Sb	Zn	Mo	Ca	Total
		mg/kg	mg/kg	mg/kg	mg/kg	mg/kg	wt%	wt%	wt%
DEP-1	45–46	5935	4690	15,050	<0.5	755	23	15	41
DEP-1	47–48	472	3216	17,640	34	1312	42	21	66

Table 3
Amounts of Mo and As mobilized from the aquifer matrix sediments by reaction with NaOAc at pH 8.1 compared to total Mo and As.

Core	Sample	Mo^A	Mo^A	Mo^T	As^A	As^A	As^T
		mg/kg	%	mg/kg	mg/kg	%	mg/kg
DEP-1	45–46	114	94	122	11	39	30
DEP-1	46–47	750	91	825	72	50	144
DEP-1	70–71	399	80	499	28	22	132
DEP-2	10–11	1	4	25	n.d.	n.d.	29
DEP-2	18–19	21	55	38	n.d.	n.d.	18
DEP-2	31–32	52	97	53	3	29	9
DEP-2	42–43	76	98	78	4	21	20
DEP-5	50–51	30	83	36	2	6	30
DEP-5	69–70	6	20	30	n.d.	n.d.	60
DEP-5	75–76	85	62	136	2	3	52

Note: Mo^A is mobilized Mo and Mo^T is total Mo in the sample; the same for As; n.d. = not detected.

et al., 2008). Of the two possible sources OM is considered the dominant source for Mo (Chappaz et al., 2014). A closer look at the element distribution in core DEP-2 (Fig. 7) corroborates OM in the sense that hydrous ferric oxide and pyrite are excluded as major sources. If those two minerals were a source for Mo then either Fe or S or both should have been elevated at depth of 40 m where Mo has its maximum concentration. Pyrite was also ruled out because no Mo was detected during the electron microprobe analyses of pyrite.

5.2. Arsenic

In the aquifer matrix below the town of Lithia in central Florida cores, As was elevated in certain horizons, particularly at depths of approximately 10 m, 45 m, 60 m and 70 m below surface in all three cores (Fig. 4). Values were comparable for all three cores with maximum values above 100 mg/kg and median values of around 3 mg/kg. These values are higher than what is considered the mean concentration of As in the Earth's crust of around 1–2 mg/kg (Li, 2000). The observed distribution and concentration values are similar to previous studies of As occurrence in the Floridan Aquifer System (FAS) (Lazareva and Pichler, 2007; Pichler et al., 2011). According to Taylor and McLennan (Taylor and McLennan, 1985) the abundance of As in the upper continental crust is approximately 1.5 ppm. This value is somewhat controversial, because most of the individual rock types that were analyzed for As have higher values. The mean abundance in the common igneous rocks, basalt and granite, are 8.3 and 7.6 ppm, respectively (Taylor, 1964). The average for shale and its related materials, such as loess and mud, is approximately 10.6 ppm (Li, 2000). The average composition for sandstone is too difficult to determine, but the value for the commonly used geostandard GSR-4 is 9.1 ppm (Govindaraju, 1994). The average value for limestone/dolomite is 2.6 ppm (Baur and Onishi, 1969). Arsenic is considered a chalcophile element and therefore often found in As-rich pyrite, although discrete As minerals, such as arsenopyrite and reaglar are common if As concentrations are sufficiently high (e.g., Borba et al., 2003; Price et al., 2013; Price and Pichler, 2006). In oxic sediments As shows a high affinity for adsorption or co-precipitation with hydrous ferric oxide (HFO), such as ferrihydrite, goethite and hematite (Dixit and Hering, 2003; Lenoble et al., 2002; Pierce and Moore, 1982).

In the subsurface As was found as a minor element in pyrite and powellite (Tables 1 and 2), while in the SAS where the conditions are more oxygenated, As was likely bound to HFO, hence the association of As and Fe (Fig. 8). In the IAS, As occurs together with powellite and in the UFA where Fe and S were elevated As should predominantly occur in As-rich pyrite. This inferred As mineralogy follows the expected redox gradient for groundwater from

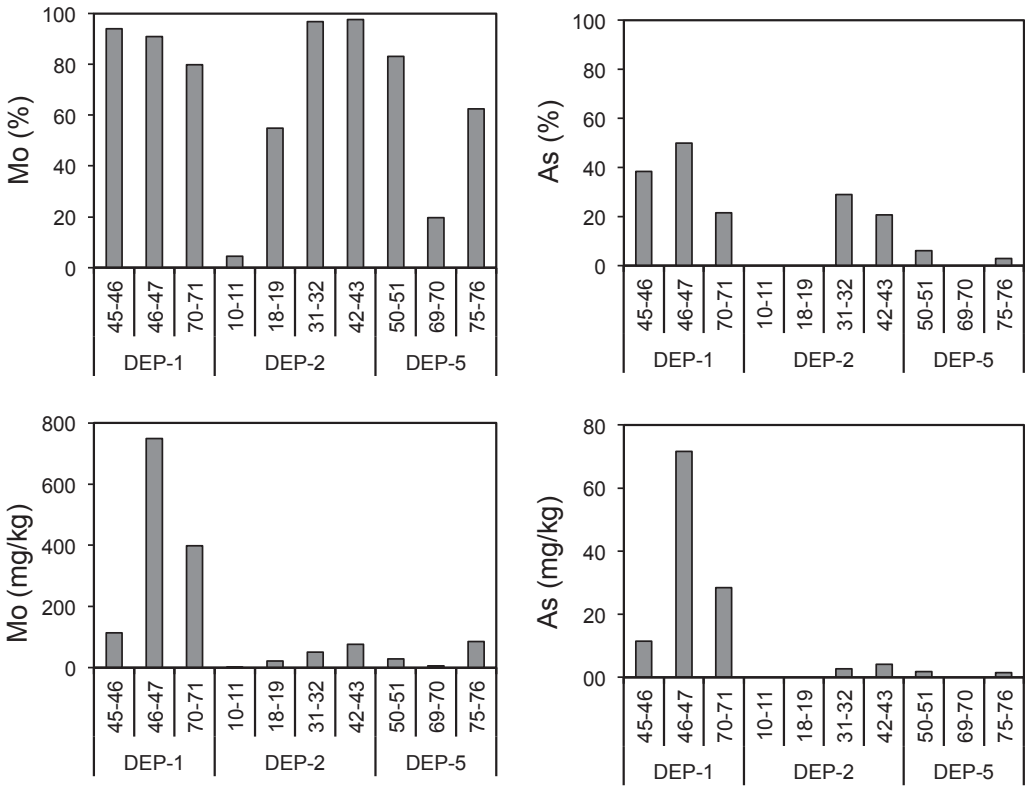

Fig. 7. Percentage and absolute amount of Mo and As mobilized during the reaction with a NaOAc solution at pH 8.1. The data corresponds to Table 3.

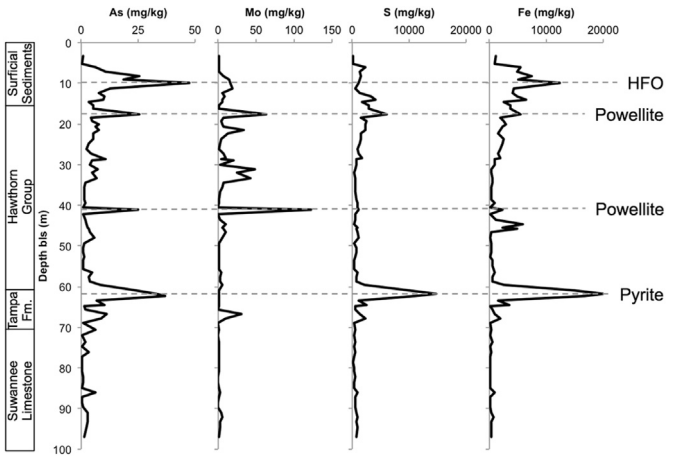

Fig. 8. Stratigraphy and depth profiles for the concentration of arsenic (As), molybdenum (Mo), sulfur (S) and iron (Fe) in core DEP-2. The dashed lines are an aid to correlate peaks across the graph and the minerals names on the right side indicate the possible source.

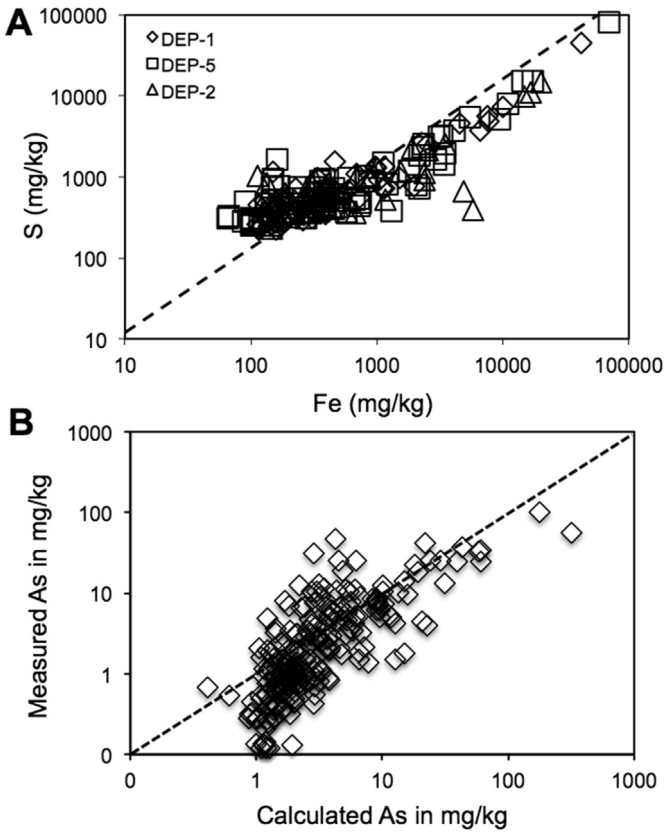

Fig. 9. (A) Plot of Fe vs. S for the three monitoring well clusters DEP-1, DEP-2 and DEP-5. The dashed line represents the "pyrite line", i.e., if pyrite would be the single source of Fe and S in a sample then all analyses would plot on this line. (B) Plot of As measured vs. As calculated, based on As abundance in pyrite (see text for more explanation). The dashed line represents the ideal case of As measured = As calculated. Data points that fall above this line contain more bulk As than expected, considering pyrite as the only source of As, and are made up of mostly samples containing clay. Data points below the line are due to high S contents in organic material and therefore have higher calculated As values.

oxygenated near the surface to more reducing conditions at depth. HFO is generally stable under oxygen-rich conditions (Jambor and Dutrizac, 1998), while pyrite is stable under the reduced conditions in the UFA (e.g., Jones and Pichler, 2007). The redox stability of powellite is not well known, however, reducing (sulfidic) conditions seem to have little influence on powellite stability, since powellite and pyrite coexist in close proximity (Fig. 6B). Unfortunately there is nothing known about abiotic molybdate reduction but sulfate its structural analog is well studied and abiotic sulfate reduction can only proceed at temperatures above 160 °C (Machel, 2001). It appears, however, that pyrite is the primary source of As in the subsurface below Lithia, because only little powellite was present in the aquifer matrix. This assumption can be verified with a massbalance approach using the bulk concentrations of Fe, S, and As combined with As concentrations in individual pyrites. Due to the correlation between S and Fe ($R^2 = 0.94$), it can be assumed that Fe and S concentrations were controlled largely by the presence of pyrite (Fig. 9A). The pyrite line (Fe = 2S) represents Fe/S ratios that are exclusively controlled by the presence of pyrite (Fig. 9A). Thus, using the values of S and Fe, the abundance of pyrite in each sample was calculated and the calculated amount of pyrite was multiplied by the mean arsenic concentration of pyrite obtained by electron microprobe analyses (Table 1) and compared to the actual analyzed bulk arsenic concentrations (Appendix A). Calculated and measured arsenic are compared in Fig. 9B. Many samples show good agreement between the measured and calculated As concentrations, i.e., they follow the dashed line in Fig. 9B. For those samples that lie significantly above the equal concentration line, calculated arsenic concentrations were lower than those measured in the bulk sample. These results can be explained by existence of other As sources such as, clays, organic material, hydrous ferrous oxides and powellite or an underestimation of the amount of pyrite. Samples that show a much higher calculated arsenic concentration compared to a measured result probably due to overestimation of pyrite abundance due to the presence of S from sources other than pyrite, e.g., gypsum or anhydrite.

5.3. Mobilization of As and Mo

Until present, no effort was made to investigate the geogenic or anthropogenic mobilization of Mo from sedimentary rocks and its impact on groundwater quality. In anoxic/sulfidic sediments, Mo is mainly associated with iron sulfides and/or OM (Chappaz et al., 2014; Dahl et al., 2013; Erickson and Helz, 2000; Glass et al., 2013; Zheng et al., 2000). In normal seawater, Mo is stable as MoO_4^{2-} with a resident time of approximately 440 thousand years (Miller et al., 2011). Its enrichment is much lower compared to sulfidic sediments and it can be preserved in marine oxic sediments by adsorption onto Fe/Mn-oxyhydroxides (Goldberg et al., 2009; Zheng et al., 2000).

Considering how As and Mo are bound in the aquifer matrix below Lithia (i.e., organic matter, pyrite, powellite and HFO; Fig. 8), changing the physicochemical conditions should cause the mobilization of As and Mo in three ways: i) the introduction of oxygen into the aquifer could result in the oxidation of pyrite and organic matter (e.g., Alberic and Lepiller, 1998); ii) consumption of oxygen by biotic and abiotic processes could result in the reduction of HFO (Amirbahman et al., 1997; Welch and Lico, 1998); and iii) non-equilibrium saturation could eventually lead to the aqueous dissolution of powellite (e.g., Conlan et al., 2012). On the other hand, the same three scenarios could also cause the precipitation of As and Mo: i) the introduction of oxidative conditions could result in the adsorption of As onto newly precipitated HFO (e.g., Pichler et al., 1999); ii) the change to reducing conditions could result in the incorporation of As into newly precipitated pyrite (Bostick and Fendorf, 2003) or adsorption of As and Mo onto pyrite (Bostick et al., 2003); and iii) non-equilibrium

saturation could result in the precipitation of powellite from super-saturated groundwater (e.g., Conlan et al., 2012). Any of these changes in the physicochemical conditions beneath Lithia can be caused by mixing between shallow, oxygenated and deep, oxygen-depleted groundwater. In Lithia each home has its own water well, because the township is not connected to the public water supply system. Thus there is the potential that the abundance of private supply wells in this area may short-circuit the hydraulic gradient across the confining layer in the Hawthorne group (IAS), e.g., bringing oxygen-depleted water from the deep aquifer into the shallow aquifer and vice versa. While there is little known about Mo mobilization, there is abundant knowledge about the release of geogenic As under oxidizing, as well as reducing conditions. Since Mo can be present in similar solid phases, such as HFO, pyrite and organic matter (e.g., Tribovillard et al., 2004), the release mechanisms of As should be a good analog. For example, Delemos et al. (2006) argued that leakage of organic contaminants from a landfill in New England, USA mobilized geogenic As by driving the reduction of As-bearing oxides. At other sites, pumping-induced hydraulic gradient changes can perturb physiochemical conditions in the aquifer, mobilizing geogenic As. Harvey et al. (2006) argue that geogenic As at their field site in Bangladesh is mobilized because pumping for irrigation draws fresh organic carbon into the aquifer, which subsequently drives the reduction of As-bearing oxides. The introduction of oxygen-rich surface water into an anoxic aquifer during aquifer storage and recovery (ASR) caused the dissolution of As-rich pyrite and thus increased As concentration in recovered water above the drinking water limit of 10 μg/L (e.g., Wallis et al., 2011). Since in an anoxic aquifer the inferred association of Mo is with organic matter (e.g., Tribovillard et al., 2004), the introduction of oxygen into an anoxic aquifer would oxidize the organic matter and liberate Mo.

From the leaching experiment it becomes clear that Mo should be easier mobilized from the aquifer matrix than As (Fig. 7). Up to 90% of Mo were removed during the reaction with 1.0 M sodium acetate (NaOAc) adjusted to a pH of 8.1, while at the same time only up to 50% As were mobilized. This indicates that the majority of Mo in the aquifer matrix is adsorbed onto mineral surfaces and organic matter, while As should be present as impurities in minerals, i.e., As in pyrite and powellite and co-precipitated with HFO. Thus the mobilization of Mo can proceed along several pathways, which are oxidation of organic matter, desorption from mineral surfaces and re-dissolution of powellite. However, only Mo mobilized through oxidation of organic matter should be considered primary Mo. There was evidence for redox disequilibrium in the IAS in the study area, i.e., co-occurrence of pyrite and HFO and pyrite and powellite in the aquifer matrix (Fig. 2). Thus, following the initial release from the aquifer matrix Mo could be adsorbed by either pyrite or HFO under uncertain redox conditions and later released from either. Since its stability is mainly controlled by the ion activity product (IAP) of Ca^{2+} and MoO_4^{2-} dissolution of secondary powellite is possible once the IAP of the groundwater is less than the K_{sp} (e.g., Conlan et al., 2012). Thus we propose that the release of Mo to groundwater in the IAS intervals could be a combination of changing redox conditions and changing ion activity product (IAP) due to mixing between shallow and deep groundwater, as well as the reversal from oxygenated to reducing conditions. Considering the observed redox disequilibrium, which indicated at least a single but most likely several redox changes, As should be mobilized similarly. During the infiltration of oxygenated surface water pyrite oxidation causes the release of As, while during periods of upward flow of oxygen-depleted groundwater, HFO is reduced and co-precipitated (sorbed) As is released.

6. Summary and conclusions

Arsenic (As) and molybdenum (Mo) were found at elevated levels in the aquifer matrix of the Surficial Aquifer System (SAS) and the Intermediate Aquifer System (IAS). Median values for both were approximately 3–6 times higher that their respective crustal averages. In the upper part of the Upper Floridan Aquifer System (UFA) median values were below their corresponding crustal averages. Thus the distribution of As and Mo in the study area seems to be controlled by the clastic and clay content of the aquifer matrix. With depth the aquifer matrix changes from (1) poorly indurated clastic deposits, to (2) interlayered sequences of carbonates, sands and clays and to (3) limestone and dolomite. That lithological change was also observed in the bulk sediment chemical composition, where Ca, Mg and Sr concentrations increased with depth, while Si, Al and P concentrations decreased with depth.

In the SAS As mainly occurred adsorbed onto hydrous ferric oxide (HFO) and in the IAS and UFA As was found as an impurity in pyrite, with concentrations of up to 9000 mg/kg. Although Mo generally has a high affinity for incorporation into pyrite, in the study area pyrite was virtually Mo-free. Thus pyrite formed during a period when Mo was either not present in the aquifer matrix or when physic-chemical conditions were such that Mo was securely bound by organic matter. In a few samples the mineral powellite ($CaMoO_4$) was discovered, which was not considered a source of Mo, but rather a sink. Geochemical modeling indicated that in the study area powellite was supersaturated and its crystal habit dismissed precipitation during sediment deposition or early diagenesis. Thus organic matter is the likely primary source of Mo in the aquifer matrix. The difference of where and how Mo and As were present in the aquifer matrix impacted their behavior during the mobilization experiments. Molybdenum, which seemed to be loosely bound to mineral and organic matter surfaces, was easily removed from the aquifer matrix. Arsenic on the other hand was much less mobile, because it occurred either tightly absorbed by HFO or as an impurity in pyrite.

Currently this study stands alone and thus it remains questionable if Mo is of similar concern as As, nevertheless it would be advisable to include Mo in the analytical program whenever elevated As concentrations are encountered in aquifers of marine origin.

Acknowledgments

We thank the Florida Department of Environmental Protection Site Investigation Section for making this study possible. Particularly the participation and support by Robert Cilek, Jeff Newton and William Martin was greatly appreciated. Olesya Lazareva, Daniela Stebbins, Angela Dippold, David Budd and Bastian Kuehl are thanked for their participation in the laboratory analyses and core descriptions. This project was partially funded by the German Research Foundation (DFG-Projekt PI 746/1-1).

Appendix A. Supplementary data

Supplementary data related to this article can be found at http://dx.doi.org/10.1016/j.apgeochem.2015.08.006.

References

Adelson, J.M., Helz, G.R., Miller, C.V., 2002. Reconstructing the rise of recent coastal anoxia; molybdenum in Chesapeake Bay sediments. Geochim. Cosmochim. Acta 66, 4367.

Ahmed, M.F., Ahuja, S., Alauddin, M., Hug, S.J., Lloyd, J.R., Pfaff, A., Pichler, T., Saltikov, C., Stute, M., van Geen, A., 2006. Ensuring safe drinking water in

Bangladesh. Science 314, 1687–1688.
Alberic, P., Lepiller, M., 1998. Oxydation de la matière organique dans un système hydrologique karstique alimenté par des pertes fluviales (Loiret, France) (Oxidation of organic matter in a karstic hydrologic unit supplied through stream sinks (Loiret, France)). Water Res. 32, 2051–2064.
Amini, M., Abbaspour, K.C., Berg, M., Winkel, L., Hug, S.J., Hoehn, E., Yang, H., Johnson, C.A., 2008. Statistical modeling of global geogenic arsenic contamination in groundwater. Environ. Sci. Technol. 42, 3669–3675.
Amirbahman, A., Sigg, L., Gunten, U.V., 1997. Reductive dissolution of Fe(III) (hydr) oxides by cysteine: kinetics and mechanism. J. Colloid Interface Sci. 194, 194–206.
Arthur, J.D., Dabous, A.A., Fischler, C., 2007. Aquifer storage and recovery in Florida: geochemical assessment of potential storage zones. In: Fox, P. (Ed.), Management of Aquifer Recharge for Sustainability, Proceedings of the International Symposium on Managed Aquifer Recharge, Scottsdale, Arizona.
Baur, W.H., Onishi, B.H., 1969. Arsenic. In: Wedepohl, K.H. (Ed.), Handbook of Geochemistry. Springer Verlag, Berlin, pp. A1–A33.
Bertine, K.K., Turekian, K.K., 1973. Molybdenum in marine deposits. Geochim. Cosmochim. Acta 37, 1415–1434.
Borba, R.P., Figueiredo, B.R., Matschullat, J., 2003. Geochemical distribution of arsenic in waters, sediments and weathered gold mineralized rocks from iron quadrangle, Brazil. Environ. Geol. 44, 39–52.
Bostick, B.C., Fendorf, S., 2003. Arsenite sorption on troilite (FeS) and pyrite (FeS2). Geochim. Cosmochim. Acta 67, 909–921.
Bostick, B.C., Fendorf, S., Helz, G.R., 2003. Differential adsorption of molybdate and tetrathiomolybdate on pyrite (FeS2). Environ. Sci. Technol. 37, 285–291.
Calvert, S.E., Pedersen, T.F., 1993. Geochemistry of recent oxic and anoxic marine sediments: implications for the geological record. Mar. Geol. 113, 67–88.
Chappaz, A., Lyons, T.W., Gregory, D.D., Reinhard, C.T., Gill, B.C., Li, C., Large, R.R., 2014. Does pyrite act as an important host for molybdenum in modern and ancient euxinic sediments? Geochim. Cosmochim. Acta 126, 112–122.
Conlan, M.J.W., Mayer, K.U., Blaskovich, R., Beckie, R.D., 2012. Solubility controls for molybdenum in neutral rock drainage. Geochem. Explor. Environ. Anal. 12, 21–32.
Crusius, J., Calvert, S., Pedersen, T., Sage, D., 1996. Rhenium and molybdenum enrichments in sediments as indicators of oxic, suboxic and sulfidic conditions of deposition. Earth Planet. Sci. Lett. 145, 65–78.
Dahl, T.W., Chappaz, A., Fitts, J.P., Lyons, T.W., 2013. Molybdenum reduction in a sulfidic lake: evidence from X-ray absorption fine-structure spectroscopy and implications for the Mo paleoproxy. Geochim. Cosmochim. Acta 103, 213–231.
Davies, T.D., Pickard, J., Hall, K.J., 2005. Acute molybdenum toxicity to rainbow trout and other fish. J. Environ. Eng. Sci. 4, 481–485.
Delemos, J.L., Bostick, B.C., Renshaw, C.E., Stürup, S., Feng, X., 2006. Landfill-stimulated iron reduction and arsenic release at the Coakley superfund site (NH). Environ. Sci. Technol. 40, 67–73.
Dixit, S., Hering, J.G., 2003. Comparison of arsenic(V) and arsenic(III) sorption onto iron oxide minerals: implications for arsenic mobility. Environ. Sci. Technol. 37, 4182–4189.
Erickson, B.E., Helz, G.R., 2000. Molybdenum(VI) speciation in sulfidic waters: stability and lability of thiomolybdates. Geochim. Cosmochim. Acta 64, 1149–1158.
Ferguson, J.F., Gavis, J., 1972. A Review of the Arsenic Cycle in Natural Waters, 6. Water Research Pergamon Press, pp. 1259–1274.
Gehman Jr., H.M., 1962. Organic matter in limestones. Geochim. Cosmochim. Acta 26, 885–897.
Glass, J.B., Chappaz, A., Eustis, B., Heyvaert, A.C., Waetjen, D.P., Hartnett, H.E., Anbar, A.D., 2013. Molybdenum geochemistry in a seasonally dysoxic Mo-limited lacustrine ecosystem. Geochim. Cosmochim. Acta 114, 204–219.
Goldberg, T., Archer, C., Vance, D., Poulton, S.W., 2009. Mo isotope fractionation during adsorption to Fe (oxyhydr)oxides. Geochim. Cosmochim. Acta 73, 6502–6516.
Govindaraju, K., 1994. 1994 compilation of working values and and sample description for 383 geostandards. Geostand. Newsl. 18, 1–158.
Green, R., Arthur, J.D., DeWitt, D., 1995. Lithostratigraphic and Hydrostratigraphic Cross Sections Through Pinellas and Hillsborough Counties, Southwest Florida. United States Geological Survey Open File Report, p. 26.
Harvey, C.F., Ashfaque, K.N., Yu, W., Badruzzaman, A.B.M., Ali, M.A., Oates, P.M., Michael, H.A., Neumann, R.B., Beckie, R., Islam, S., Ahmed, M.F., 2006. Groundwater dynamics and arsenic contamination in Bangladesh. Chem. Geol. 228, 112–136.
Hatch, J.R., Leventhal, J.S., 1992. Relationship between inferred redox potential of the depositional environment and geochemistry of the upper Pennsylvanian (Missourian) stark shale member of the Dennis limestone, Wabaunsee Country, Kansas, U.S.A. Chem. Geol. 99, 65–82.
Heijerick, D.G., Regoli, L., Carey, S., 2012. The toxicity of molybdate to freshwater and marine organisms. II. Effects assessment of molybdate in the aquatic environment under REACH. Sci. Total Environ. 435, 179–187.
Helz, G.R., Bura-Nakić, E., Mikac, N., Ciglenečki, I., 2011. New model for molybdenum behavior in euxinic waters. Chem. Geol. 284, 323–332.
Helz, G.R., Miller, C.V., Charnock, J.M., Mosselmans, J.F.W., Pattrick, R.A.D., Garner, C.D., Vaughan, D.J., 1996. Mechanism of molybdenum removal from the sea and its concentration in black shales: EXAFS evidence. Geochim. Cosmochim. Acta 60, 3631–3642.
Hughes, J.D., Vacher, H.L., Sanford, W.E., 2009. Temporal response of hydraulic head, temperature, and chloride concentrations to sea-level changes, Floridan aquifer system, USA. Hyrogeol. J. 17, 793–815.
Jambor, J.L., Dutrizac, J.E., 1998. Occurrence and constitution of natural and synthetic ferrihydrite, a widespread iron oxyhydroxide. Chem. Rev. 98, 2549–2585.
Jenne, E.A., 1998. Adsorption of Metals by Geomedia: Variables, Mechanisms, and Model Applications. Academic Press, San Diego.
Jones, G.W., Pichler, T., 2007. The relationship between pyrite stability and arsenic mobility during aquifer storage and recovery in southwest central Florida. Environ. Sci. Technol. 41, 723–730.
Katz, B.G., Crandall, C.A., Metz, P.A., McBride, W.S., Berndt, M.P., 2007. Chemical Characteristics, Water Sources and Pathways, and Age Distribution of Ground Water in the Contributing Recharge Area of a Public-supply Well Near Tampa, Florida, 2002–05. USGS Scientific Investigations Report 2007-5139, 85 pp.
Katz, B.G., McBride, W.S., Hunt, A.G., Crandall, C.A., Metz, P.A., Eberts, S.M., Berndt, M.P., 2009. Vulnerability of a public supply well in a karstic aquifer to contamination. Ground Water 47, 438–452.
Korte, N.E., Fernando, Q., 1991. A review of arsenic(III) in groundwater. Crit. Rev. Environ. Control 21, 1–36.
Lazareva, O., Pichler, T., 2007. Naturally occurring arsenic in the Miocene hawthorn group, Southwestern Florida: implication for phosphate mining. Appl. Geochem. 22, 953–973.
Lenoble, V., Bouras, O., Deluchat, V., Serpaud, B., Bollinger, J.-C., 2002. Arsenic adsorption onto pillared clays and iron oxides. J. Colloid Interface Sci. 255, 52–58.
Li, Y.-H., 2000. A Compendium of Geochemistry: from Solar Nebula to the Human Brain. Princeton University Press, Princeton.
Machel, H.-G., 2001. Bacterial and thermochemical sulfate reduction in diagenetic settings – old and new insights. Sediment. Geol. 140, 143–175.
McNeill, L.S., Hsiao-wen, C., Edwards, M., 2002. Aspects of arsenic chemistry in relation to occurrence, health and treatment. In: Frankenberger Jr., W.T. (Ed.), Environmental Chemistry of Arsenic. Marcel Dekker, New York, pp. 141–154.
Miller, C.A., Peucker-Ehrenbrink, B., Walker, B.D., Marcantonio, F., 2011. Re-assessing the surface cycling of molybdenum and rhenium. Geochim. Cosmochim. Acta 75, 7146–7179.
Miller, J.A., 1986. Hydrogeologic Framework of the Floridan Aquifer System in Florida, Georgia, South Carolina and Alabama.
Peters, S.C., Blum, J.D., 2003. The source and transport of arsenic in a bedrock aquifer, New Hampshire, USA. Appl. Geochem. 18, 1773–1787.
Pichler, T., 2005. $\delta^{34}S$ isotope values of dissolved sulfate (SO_4^{2-}) as a tracer for battery acid (H_2SO_4) contamination. Environ. Geol. 47, 215–224.
Pichler, T., Hendry, J., Hall, G.E.M., 2001. The mineralogy of arsenic in uranium mine tailings at the Rabbit Lake in-pit facility, Northern Saskatchewan, Canada. Environ. Geol. 40, 495–506.
Pichler, T., Price, R.E., Lazareva, O., Dippold, A., 2011. Determination of arsenic concentration and distribution in the Floridan aquifer System. J. Geochem. Explor. 111, 84–96.
Pichler, T., Sültenfuß, J., 2010. A stable and radioactive isotope study of geogenic arsenic contamination in a limestone aquifer. In: Levin, C., Grathwohl, P., Kappler, A., Kaufmann-Knoke, R., Rügner, H. (Eds.), Grundwasser für die Zukunft. E. Schweizerbart, Tübingen, p. 62.
Pichler, T., Veizer, J., Hall, G.E.M., 1999. Natural input of arsenic into a coral-reef ecosystem by hydrothermal fluids and its removal by Fe(III) oxyhydroxides. Environ. Sci. Technol. 33, 1373–1378.
Pierce, M.L., Moore, C.B., 1982. Adsorption of arsenite and arsenate on amorphous iron hydroxide. Water Res. 16, 1247–1253.
Price, R.E., S, I., Planer-Friedrich, B., Bühring, S.I., Amend, J., Pichler, T., 2013. Processes influencing extreme As enrichment in shallow-sea hydrothermal fluids of Milos Island, Greece. Chem. Geol. 348, 15–26.
Price, R.E., Pichler, T., 2005. Distribution, speciation and bioavailability of arsenic in a shallow-water submarine hydrothermal system, Tutum Bay, Ambitle Island, PNG. Chem. Geol. 224, 122–135.
Price, R.E., Pichler, T., 2006. Abundance and mineralogical association of arsenic in the Suwannee limestone (Florida): implications for arsenic release during water–rock interaction. Chem. Geol. 228, 44–56.
Price, W.A., Hart, B., Howell, C., 1999. Proceedings of the 1999 Workshop on Molybdenum Issues in Reclamation. British Columbia Technical and Research Committee on Reclamation, p. 144.
Riggs, S.R., 1984. Paleoceanographic model of Neogene phosphorite deposition, U.S. Atlantic Continental margin. Science 223, 123–131.
Scott, T.M., 1988. Lithostratigraphy of the hawthorn group (Miocene) of Florida. Fla. Geol. Surv. Bull. 1–148.
Scott, T.M., 1990. The Lithostratigraphy of the Hawthorn Group of Peninsular Florida. Florida Geologica Survey Open File Report 36, Open file report. FGS.
Smedley, P.L., Cooper, D.M., Ander, E.L., Milne, C.J., Lapworth, D.J., 2014. Occurrence of molybdenum in British surface water and groundwater: distributions, controls and implications for water supply. Appl. Geochem. 40, 144–154.
Taylor, S.R., 1964. Abundance of elements in the crust: a new table. Geochim. Cosmochim. Acta 28, 1273–1285.
Taylor, S.R., McLennan, S.M., 1985. The Continental Crust: Its Composition and Evolution. Blackwell Scientific Publications, Oxford.
Tribovillard, N., Lyons, T.W., Riboulleau, A., Bout-Roumazeilles, V., 2008. A possible capture of molybdenum during early diagenesis of dysoxic sediments. Bull. De. La Soc. Geol. De. Fr. 179, 3–12.
Tribovillard, N., Riboulleau, A., Lyons, T., Baudin, F., 2004. Enhanced trapping of molybdenum by sulfurized marine organic matter of marine origin in Mesozoic limestones and shales. Chem. Geol. 213, 385–401.

van der Veen, N.G., Keukens, H.J., Vos, G., 1985. Comparison of ten digestion procedures for the determination of arsenic in soils by hydride-generation atomic absorption spectrometry. Anal. Chim. Acta 171, 285–291.
Wallis, I., Prommer, H., Pichler, T., Post, V., Norton, S.B., Annable, M.D., Simmons, C.T., 2011. Process-based reactive transport model to quantify arsenic mobility during aquifer storage and recovery of potable water. Environ. Sci. Technol. 45, 6924–6931.
Welch, A.H., Lico, M.S., 1998. Factors controlling As and U in shallow ground water, southern Carson Desert, Nevada. Appl. Geochem. 13, 521–539.
WHO, 2011. Guidelines for Drinking-water Quality, fourth ed. World Health Organization, Geneva.
Zhai, X.W., Zhang, Y.L., Qi, Q., Bai, Y., Chen, X.L., Jin, L.J., Ma, X.G., Shu, R.Z., Yang, Z.J., Liu, F.J., 2013. Effects of molybdenum on sperm quality and testis oxidative stress. Syst. Biol. Reprod. Med. 59, 251–255.
Zheng, Y., Anderson, R.F., van Geen, A., Kuwabara, J., 2000. Authigenic molybdenum formation in marine sediments: a link to pore water sulfide in the Santa Barbara Basin. Geochim. Cosmochim. Acta 64, 4165–4178.